Journal of Thermal Analysis and Calorimetry
https://doi.org/10.1007/s10973-025-14691-x

Energy and exergy analysis of a cycle-skipping strategy in an HCCI engine fueled with natural gas

Nisa Nur Atak[1] · Erdal Tunçer[2] · Battal Doğan[3] · Kenan Ünal[4]

Received: 12 April 2025 / Accepted: 8 August 2025

Abstract
Homogeneous charge compression ignition (HCCI) engines have attracted considerable interest due to its incorporation of features from both gasoline and diesel engines. In this study, the effects of cycle-skipping strategies on engine performance, efficiency, and emissions in a natural gas-fired HCCI engine were investigated experimentally. Experiments were conducted under constant engine speed, at 25, 50, and 75% load levels, in the Normal, 3 Normal-1 Skip (3N1S), 2 Normal-1 Skip (2N1S), and 1 Normal-1 Skip (1N1S) cycle modes. Emissions, fuel consumption, energy–exergy flow, thermal losses, irreversibilities, entropy generation, thermal, and exergy efficiencies were calculated based on the experimental data. Under 50% engine load, the NOx emission in the 3N1S operating mode was measured at 1594 ppm, whereas it increased by 52.5% to 2431 ppm in the 2N1S mode. The correlation between cycle-skipping tactics and thermal efficiency was determined to be contingent upon engine load. In Normal and 3N1S modes, thermal efficiency generally improves with elevated engine loads, while the 2N1S and 1N1S modes provide superior performance at low to medium loads. At a constant 50% load, heat efficiency in the 2N1S mode increased by 7.84% to reach 28.34% compared to the Normal mode. Additionally, thermodynamic analyses revealed that the 1N1S mode has the lowest entropy generation and the least irreversibility, at 0.021 kW/K. These results demonstrate that cycle-skipping strategies can be an effective tool for optimizing engine performance based on load.

Keywords Cycle skipping · HCCI · Natural gas · Energy · Exergy

Introduction

Energy is fundamental to contemporary societal advancement and sustainability. Since the Industrial Revolution, technological and industrial improvements have resulted in a persistent rise in worldwide energy demand [1–3]. The effective use of energy resources has become as crucial an issue as their acquisition. Internal combustion engines (ICEs), characterized by their high energy density and versatility in fuel usage, continue to be essential in the transportation and mobility sectors. Currently, these engines are extensively utilized in several applications, such as automotive technologies, agricultural machinery, power generating, and maritime transportation [4]. Internal combustion engines transform chemical energy into mechanical energy by the regulated ignition of fuel within the combustion chamber, providing the versatility to function with many fuel types based on their core operational principles. As a result, the use of alternative fuels into internal combustion engines has become increasingly common [5–9]. The fuel type utilized in an internal combustion engine markedly affects emission levels [9, 10], engine efficiency [11, 12], and torque production [13, 14]. Natural gas, a significant alternative fuel, is extensively utilized in engines due to its abundance and reduced exhaust emissions relative to other fuels [15–17].

In Xing et al. [18], the performance and emission effects of low-carbon alternative fuel options were investigated in a marine vessel powered by an ICE. The findings indicated that the use of hydrogen and ammonia—followed by biodiesel and bioethanol—represents a viable option for marine

✉ Kenan Ünal
kenanunal@gazi.edu.tr

1 Gazi University Institute of Science, Gazi University, 06330 Ankara, Turkey

2 Mechanical Engineering, Istanbul Health and Technology University, 34445 Istanbul, Turkey

3 Energy Systems Engineering, Faculty of Technology, Gazi University, 06330 Ankara, Turkey

4 Department of Motor Vehicles and Transportation Technology, TUSAŞ Kazan Vocational School, Gazi University, 06980 Ankara, Turkey

Published online: 07 September 2025

transportation. Jayabal [19] examined the impact of a biodiesel derived from sapota seed biodiesel (SSB) and hydrogen gas blend on the operational and emission behavior of a dual-fuel CI engine. The hydrogen injection improved heat efficiency and significantly reduced emissions. The study reported an increase of 14.62% in brake thermal efficiency (BTE) and a reduction of up to 80% in emissions such as CO_2, CO, and HC. Kumar et al. [20] investigated the performance, combustion, and emission characteristics of alternative fuels produced by blending waste plastic oil (WPO) and waste cooking oil-based biodiesel (WCOB) in an internal combustion diesel engine. According to the results, the B20P20D60 blend yielded the highest efficiency and the lowest emissions among the tested fuel combinations. M'hamed et al. [21] conducted an experimental study on diesel–alcohol blends by mixing ethanol and methanol with diesel fuel at varying ratios in an ICE. The study assessed how these fuel blends impact engine performance and examined the engine's power output, emissions, and energy economy. The results indicated that incorporating ethanol and methanol into diesel fuel has the potential to reduce emissions while enhancing overall efficiency.

In light of current energy policies and sustainability objectives, ICE technologies are undergoing a substantial transformation, both in terms of engineering advancements and compliance with environmental regulations. While the rise of electric and hybrid vehicles is reshaping the future of propulsion systems, innovative strategies aimed at developing more efficient and environmentally friendly combustion processes are actively being pursued [19, 22]. Diesel CI and gasoline SI engines necessitate continuous innovation—not only in engine design, but also in ensuring compatibility with a variety of fuel types. HCCI engines are an innovative technology that combines the advantages of both gasoline and diesel ICEs. In HCCI engines, a homogeneous fuel–air mixture is auto-ignited through compression within the cylinder, eliminating the need for a spark plug or direct injection ignition systems [23, 24]. Zapata-Mina et al. [25] conducted an experimental study on a single-cylinder HCCI engine using fuel blends composed of fusel oil and diethyl ether in varying ratios (D40F60, D60F40, and D80F20). The results, obtained under different engine speeds and lambda values, revealed that increasing the proportion of diethyl ether led to a decline in performance, with the lowest exergy efficiency of 5.34% recorded for the D80F20 blend. Tunçer et al. [26] conducted an experimental study on a HCCI engine powered by natural gas and evaluated its performance against a standard SI engine. Based on the findings, it was observed that the fuel consumption of the HCCI engine was 2.92% higher than that of the SI engine. Furthermore, the NO_x emission was measured at 19.84 g/kWh for the HCCI engine, whereas it was 35.72 g/kWh for the SI engine.

Verma et al. [27] investigated the effects of various fuels on engine performance and emissions in an HCCI engine. The results indicated that the use of natural gas in HCCI operation led to at least a 10% improvement in engine efficiency compared to diesel fuel. Additionally, it was found that HCCI engines produced lower exhaust emissions relative to conventional internal combustion engine types. Çelebi et al. [28] conducted an experimental study using different ratios of naphtha blends (N25, N50, and N75) and n-heptane in a single-cylinder HCCI engine with a maximum power output of 15 kW. At a lambda (λ) value of 2, an intake air temperature of 60 °C, and an engine speed of 1400 rpm, the CO emission values for n-heptane and N75 fuels were measured as 0.048% and 0.08%, respectively. In HCCI engines, parameters such as fuel injection strategy [29–31] and compression ratio [32, 33] significantly influence engine performance and have been the subject of numerous studies.

Cycle-skipping strategy (SCS) is a method used to reduce the energy losses of the engine under low load conditions [34]. This approach dynamically regulates the effective stroke volume by deactivating specific engine valves, thereby minimizing pumping losses [35, 36]. As a result, SCS allows the engine to operate with lower energy consumption under partial load conditions, enhancing overall engine efficiency [36]. There are studies examining the effects of SCS on engine performance and emissions in various engine types [37–39]. Tunçer [40] experimentally evaluated the use of pure diesel and pure natural gas (NG100) in a single-cylinder engine under normal operation and two different SCS modes (2N1S and 3N1S) at a fixed speed of engine of 1500 rpm. Exergy and energy analyses were performed using the data. At 75% engine load, the heat efficiency was calculated as 34% in the natural gas-fueled normal cycle and 30% in the 2N1S cycle. Under 25% engine load, the exergy destruction in the 2N1S and 3N1S modes was found to be 13 kW and 16.54 kW, respectively.

The use of the skip cycle system in a four-stroke, single-cylinder, water-cooled spark ignition engine running at a steady 2000 rpm was empirically examined by Kutlar et al. [34]. The results indicated that rising the engine speed led to a significant rise in fuel consumption under cycle-skipping conditions. At 2000 rpm, the brake-specific fuel consumption (BSFC) was recorded as 680 g/kWh in the Normal mode of operation, whereas it increased to 954 g/kWh in the normal–skip–skip (NSS) mode. Tunçer et al. [41] conducted tests under three different operating conditions—Normal, 3N1S, and 2N1S—in a single-cylinder, natural gas-fueled SI engine using the skip cycle method. According to the CO emission data, the lowest CO emission was recorded under the normal operation mode, while the highest CO emission, 116 g/kWh, was recorded in the 2N1S mode. Additionally,

the engine exhibited its highest heat efficiency, 28%, under the 3N1S operating condition.

Various studies in the literature have concentrated on the performance, emissions, and thermodynamic assessments of HCCI engines. Nonetheless, there is a significant deficiency in research concerning exergy and energy studies for HCCI engines utilizing natural gas fuel under cycle-skipping conditions.

This study reveals how cycle-skipping modes in natural gas-fueled HCCI engines create a difference not only in performance but also in thermodynamic terms, and in this respect, expands the depth of technical analysis in the literature.

System components and application methodology

Data preparation

This paper involves the modification of a typical diesel engine to utilize natural gas as its primary fuel. The original diesel injector was extracted, and a spark plug was fitted into the cylinder head to enable ignition. A throttle valve and natural gas injectors were custom-manufactured and built into the system to control gas flow. Inductive sensors were fitted on the engine to measure crankshaft velocity and to ascertain the position of the top dead center (TDC). The data obtained from these sensors were processed using computer programs that are specialized.

Engine mapping revealed that the highest engine load occurred at 1500 rpm. Consequently, tests were conducted at three distinct engine loads: 75, 50, and 25%. Cycle-skipping strategies were applied by modifying ignition timing and gas injection patterns. Four operating modes were tested: Normal (N), 3 Normal–1 Skip (3N1S), 2 Normal–1 Skip (2N1S), and 1 Normal–1 Skip (1N1S). A schematic diagram of the experimental setup is presented in Fig. 1, while the technical specifications are summarized in Tables 1 and 2.

For HCCI operation, the intake air was preheated to raise the in-cylinder temperature, enabling the natural gas to reach its auto-ignition point and achieve stable combustion. Due to its higher auto-ignition temperature compared to gasoline and diesel, natural gas required intake air temperatures above 100 °C to ignite spontaneously. To ensure consistent thermal conditions during the tests, two PT100 temperature sensors were installed—one at the intake port and one before the intake valve.

Additionally, a knock sensor was mounted to monitor and prevent engine knocking. When switching to HCCI mode, the spark plug cable was disconnected to disable spark ignition. The engine was allowed to stabilize under HCCI conditions before initiating the test measurements. During the experimental studies, signals corresponding to TDC position, in-cylinder pressure, gas injection, and ignition were recorded using an oscilloscope. Emission measurements were conducted using a Bosch BEA 060 gas analyzer in accordance with the ISO 3046-1 standard. The overall experimental flowchart is illustrated in Fig. 2.

Error and uncertainty analysis

Ensuring the reliability of the study requires the verification of data obtained from engine tests. Measurement errors may arise due to factors such as instrument selection, ambient conditions, reading inaccuracies, and calibration-related uncertainties during the experiments. In this study, an uncertainty analysis was conducted to identify and minimize potential measurement errors. The accuracy levels and uncertainty values associated with the measurements are presented in Table 3.

Energy analysis

An exergy and energy analysis of an ICE was conducted to investigate its performance and emission characteristics under different operating modes is presented in Fig. 3. In this analysis, the engine is assumed to operate under steady-state conditions, and the following assumptions are applied:

- Combustion air and exhaust gases are considered ideal gases.
- Average values are used for specific heat capacities.
- Changes in kinetic and potential exergies are neglected.
- The ambient temperature and pressure are taken as 293 K and 1 atm, respectively.

The mass flow rate into the system ($\dot{m}_{in}$) is equal to the mass flow rate out of the system ($\dot{m}_{out}$) for a control volume with steady flow, as stated in Eq. (1), in accordance with the principle of mass conservation [45].

$$\sum \dot{m}_{in} = \sum \dot{m}_{out} \tag{1}$$

The difference between the energy transported by the mass entering and leaving the system equals the difference between the heat transferred to the system ($\dot{Q}$) and the work produced by the system ($\dot{W}$) [46]. The energy balance is expressed by Eq. (2).

$$\sum \dot{m}_{out} h_{out} - \sum \dot{m}_{in} h_{in} = \dot{Q} - \dot{W} \tag{2}$$

General representation of the energy conservation law for control volumes with multiple inlets and outlets is given in Eq. (3). The rate of chemical energy supplied to the engine via fuel can be calculated using Eq. (4), where H_u is the

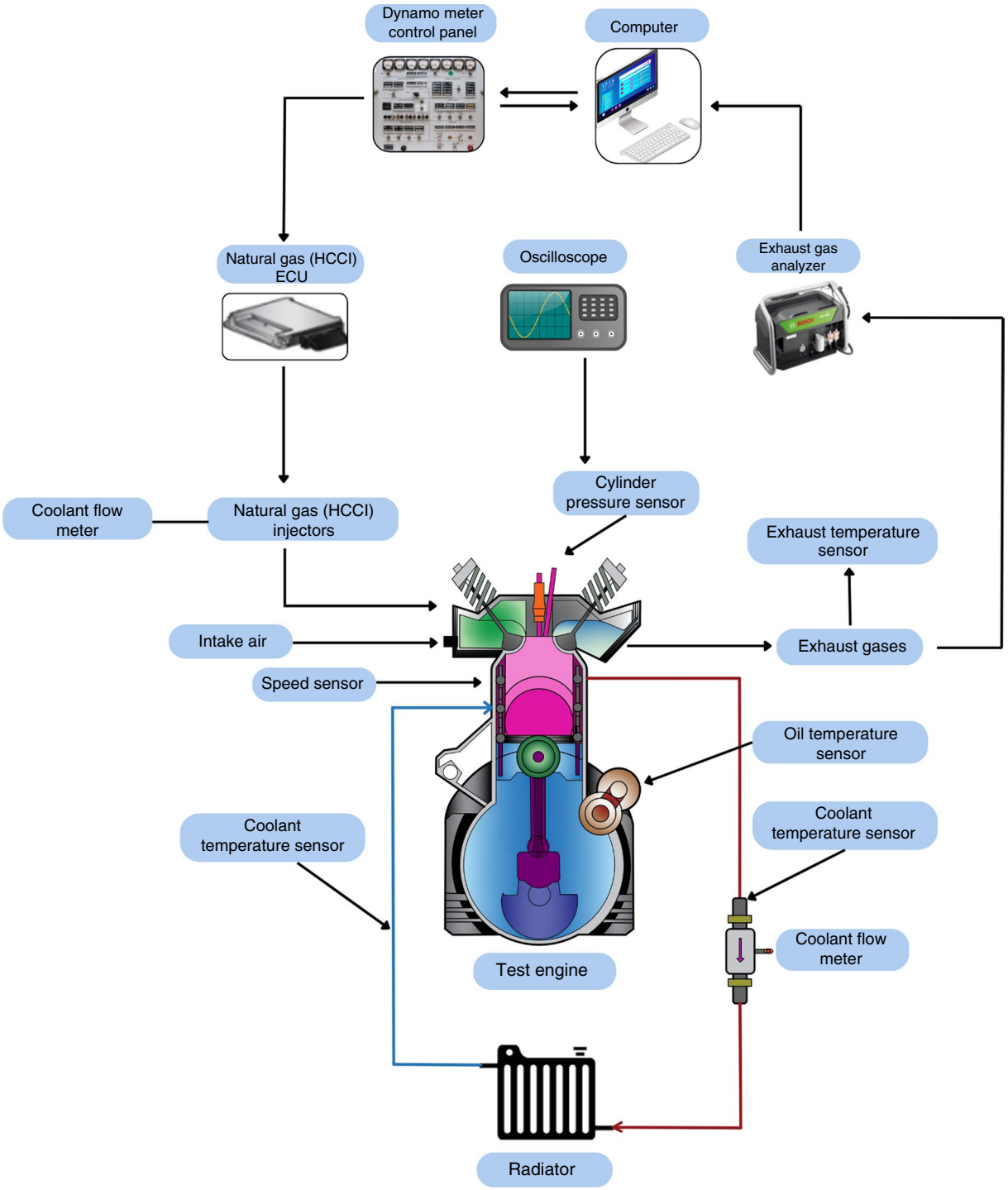

Fig. 1 Experimental setup block diagram

lower heating value of the fuel and $\dot{m}_{\text{fuel}}$ is the mass flow rate of the fuel [47].

$$\dot{Q}_{\text{in}} - \dot{Q}_{\text{out}} + \sum \dot{m}_{\text{in}} h_{\text{in}} = \dot{W}_{\text{out}} - \dot{W}_{\text{in}} + \sum \dot{m}_{\text{out}} h_{\text{out}} \tag{3}$$

$$\dot{E}_{\text{fuel}} = \dot{m}_{\text{fuel}} H_{\text{u}} \tag{4}$$

In an engine control volume, the total chemical energy of the fuel ($\dot{E}_{\text{fuel}}$) is either converted into mechanical work ($\dot{W}$) or dissipated as heat losses to the environment ($\dot{Q}_{\text{loss}}$). The relationship is expressed by Eq. (5) [48].

Table 1 Technical characteristics of the engine used in experimental studies

Parameters	Specification
Engine supplier	Erin Engine Corporation Inc
Brand	Erin Engine
Model	1.16L Diesel—1.16L Natural gas engine
Cylinder number	1
Engine cycle	4
Maximum engine power	10 kW @ 1500 rpm
Maximum engine torque	60 Nm @ 1500 rpm
Powertrain	Camshaft located in the engine with push-rod mechanism
Valve system	4 valves per cylinder
Fuel injection type	Port injection (Natural gas)
Ignition	Compression-ignition (Diesel) Electronically Spark-ignition (Natural gas)
Cooling system	Water cooled
Idle speed	1500 rpm
Swept volume	1160 cm^3
Cylinder bore	108 mm
Stroke	127 mm
Compression ratio	14.6:1
Number of injectors nozzle	6
Intake valve timing advance	25° BTDC
Intake valve closure retardation	65° ABDC
Injection timing of fuel	19° BTDC
Opening advance of exhaust valve	55° BBDC
Closing delay of exhaust valve	35° ATDC

Table 2 Technical specifications of fuels used in the experimental study [42–44]

Property	Natural gas
Fuel density at 15 °C/kg m^{-3}	0.72–0.75
Fuel viscosity/mm^2 s^{-1}	16.33
Cetane number	–
Octane number	120
Molecular weight/kg mol^{-1}	16.04
Lower calorific value/MJ kg^{-1}	46.0–48.0
Latent heat of evaporation/kJ kg^{-1}	511
Percentage of methane by volume	92.5
Percentage of ethane by volume	3
Percentage of propane by volume	0.71
Percentage of butane by volume	0.02
Percentage of pentane by volume	0.1
Percentage of carbon dioxide by volume	0.6
Percentage of nitrogen by volume	3

$$\dot{Q}_{\text{loss}} = \dot{\text{E}}_{\text{fuel}} - \dot{W} \tag{5}$$

The heat efficiency (η_{th}) is a key indicator of the energy conversion performance of the system. It represents the ratio of useful work output to the total fuel energy input and is given by Eq. (6) [47].

$$\eta_{\text{th}} = \frac{\dot{W}}{\dot{E}_{\text{fuel}}} \tag{6}$$

Exergy analysis of the system

Exergy analysis is a thermodynamic approach employed to detect irreversibilities in a system and evaluate the potential for recoverable energy, facilitating more efficient energy transfer procedures. This analysis focuses on the quality of energy and the amount of usable energy. The exergy balance for the control volume of the engine is expressed by Eq. (7), where the incoming ($\dot{E}x_{\text{in}}$) and outgoing ($\dot{E}x_{\text{out}}$) exergy flow rates are equal under ideal, reversible conditions [49].

$$\dot{E}x_{\text{in}} = \dot{E}x_{\text{out}} \tag{7}$$

In this study, the exergy of incoming air ($\dot{E}x_{\text{air}}$) is assumed to be zero, as the air is considered to enter the engine under ambient atmospheric conditions. The exergy of the fuel ($\dot{E}x_{\text{fuel}}$) is distributed into work exergy ($\dot{E}x_{\text{work}}$), exhaust gas

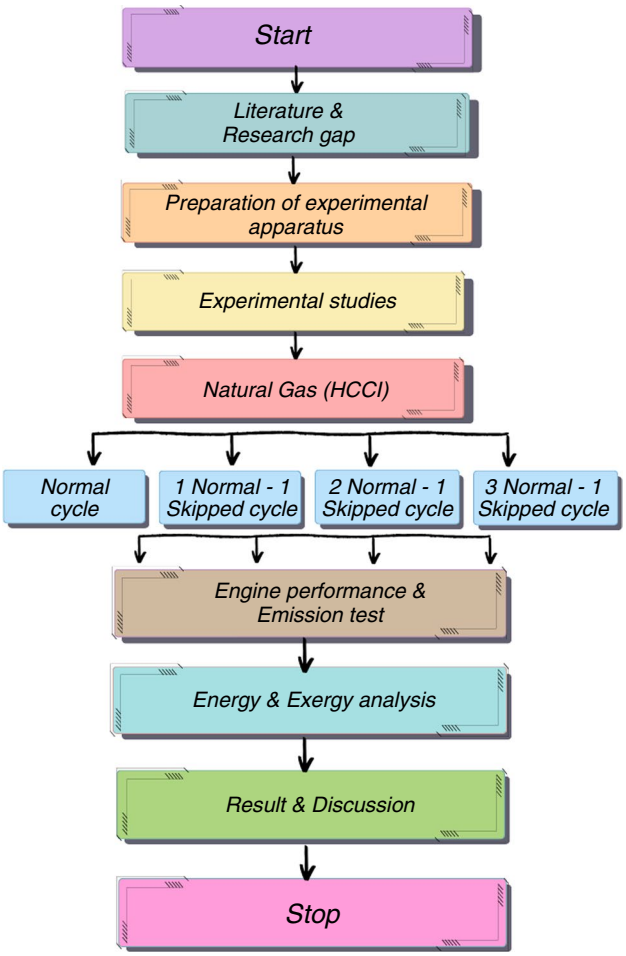

Fig. 2 General flowchart of the this study

Table 3 Inaccuracy in measured data and computational results

Parameter	Measuring range	Accuracy	Uncertainty/%
The power of engine	–	–	±0.57
The speed of engine	0–2000 rpm	±1 rpm	±0.063
BSFC	–	–	±0.762
Flow rate of Fuel	–	–	±0.41
Flow rate of Air	–	–	±0.52
Brake torque	0–50 Nm	±0.1 Nm	±0.50
Temperature	-	±0.1 °C	±1.0
NO	0–5000 ppm	±1 ppm	±0.601
O_2	0–25% vol	±0.01%	±0.561
CO	0–5% volume	±0.001%	±0.823
HC	0–3000 ppm	±1 ppm	±0.925

exergy ($\dot{E}x_{eg}$), heat losses ($\dot{E}x_{heat}$), and irreversibilities ($\dot{E}x_{dest}$) as expressed in Eq. (8) [48].

$$\dot{E}x_{air} + \dot{E}x_{fuel} = \dot{E}x_{work} + \dot{E}x_{eg} + \dot{E}x_{heat} + \dot{E}x_{dest} \quad (8)$$

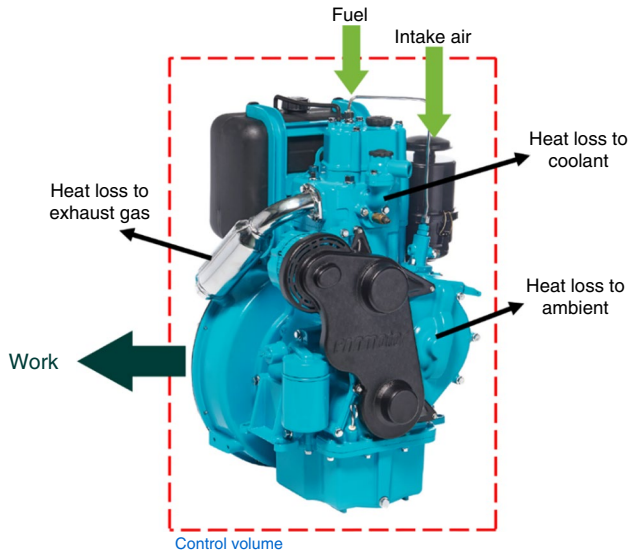

Fig. 3 Engine used in experimental studies

The elemental composition of the natural gas used in this study is as follows: hydrogen (H) 12.982%, carbon (C) 86.984%, and sulfur (S) 0.034%. Based on this composition, the exergy factor (φ) of the fuel is calculated using Eq. (9) [50].

$$\varphi = 1.033 + 0.0169\left(\frac{n}{m}\right) - \left(\frac{0.0698}{m}\right) \quad (9)$$

The specific exergy of the fuel (ε_{fuel}) is obtained by multiplying the lower heating value of the fuel ($\dot{E}x_{fuel}$) by its exergy factor [51]:

$$\varepsilon_{fuel} = H_u \varphi \quad (10)$$

$$\dot{E}x_{fuel} = \dot{m}_{fuel}\varepsilon_{fuel} \quad (11)$$

The total exergy of the exhaust gases at the engine outlet consists of two components: physical exergy (ε_{phy}) and chemical exergy (ε_{chem}). ε_{phy} is derived from the derivations in enthalpy and entropy from reference environment, while chemical exergy reflects the chemical potential of gas mixture based on its composition. The calculations are based on mole fractions (y^e) of the reference value at ambient temperature (T_0) as shown in Table 4. The total exergy of the exhaust gas is the sum of its physical and chemical exergy components and represents the overall exhaust exergy potential [52, 53].

$$\varepsilon_{phy} = \left[\left(h - T_0 s\right) - \left(h_0 - T_0 s_0\right)\right] \quad (12)$$

$$\varepsilon_{chem} = \underline{R} T_0 \ln \frac{1}{y^e} \quad (13)$$

Table 4 The elements of the environment [54]

Reference component	Mol fractions (y^e) /%
N_2	75.6700
O_2	20.3500
CO_2	0.03450
H_2O	3.03000
CO	0.00070
SO_2	0.00020
H_2	0.00005
Others	0.91455

$$\varepsilon = \varepsilon_{phy} + \varepsilon_{chem} \tag{14}$$

The exergy loss due to heat dissipation in an engine ($\dot{E}x_{heat}$) is a parameter that depends on the ambient temperature, the system temperature (T_s), and the rate of heat transfer to the environment via the cooling water ($\dot{Q}_{cw}$). This quantity is calculated to evaluate the heat losses occurring in the system. The exergy associated with heat transfer is determined using Eq. (15) [55]. The amount of heat dissipated by the cooling water ($\dot{Q}_{cw}$) is calculated using Eq. (16), based on the difference between the total fuel energy input and the sum of mechanical work output and enthalpy change of the exhaust gases.

$$\dot{E}x_{heat} = \sum \left(1 - \frac{T_0}{T_s}\right)\dot{Q}_{cw} \tag{15}$$

$$\dot{Q}_{cw} = \dot{m}_{fuel}H_u - (\dot{E}x_w + \dot{m}_{out}\Delta h_{out}) \tag{16}$$

Exergy destruction ($\dot{E}x_{dest}$) plays a critical role in evaluating system inefficiencies, as it quantifies the non-recoverable energy losses. It is calculated as the difference between the total exergy input from the fuel and the sum of useful work output, exhaust exergy, and heat loss exergy, as given in Eq. (17). Entropy generation ($\dot{s}_{gen}$) is a measure of the irreversibility and disorder introduced into the system. It is calculated by dividing the $\dot{E}x_{dest}$ by the ambient temperature, as shown in Eq. (18) [56].

$$\dot{E}x_{dest} = \dot{E}x_{fuel} - (\dot{E}x_{work} + \dot{E}x_{eg} + \dot{E}x_{heat}) \tag{17}$$

$$\dot{s}_{gen} = \frac{\dot{E}x_{dest}}{T_0} \tag{18}$$

Exergy efficiency (ψ), also referred to as the second law efficiency, is a key performance indicator for assessing irreversibilities and entropy production within the system. It is defined as the ratio of the useful exergy output (work) to the total exergy input and is expressed in Eq. (19) [57].

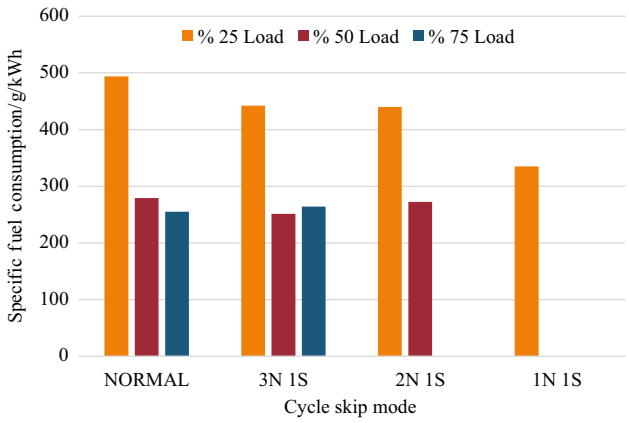

Fig. 4 Fuel consumption in HCCI engine at different engine loads and operating modes

$$\psi = \frac{\dot{E}x_w}{\dot{E}x_{in}} \tag{19}$$

A high exergy efficiency indicates that a greater portion of the input fuel exergy is effectively converted into useful work. Conversely, a low exergy efficiency suggests that a significant amount of energy is lost to the environment or consumed in irreversible processes.

Experimental results

Performance, emission, and thermodynamic analyses (energy and exergy) were conducted on a natural gas-fueled HCCI engine operating under four distinct cycle-skipping strategies (Normal, 3N1S, 2N1S, and 1N1S) and at three engine loads (25, 50, and 75%). Critical parameters such as fuel consumption, exhaust emissions, heat losses, energy and exergy flows, irreversibilities, entropy generation, heat efficiency, and exergy efficiency were evaluated based on experimental data.

Fuel consumption, which represents the mass of fuel consumed per unit output energy, is a crucial indicator for evaluating both system efficiency and environmental impact. As shown in Fig. 4, fuel consumption generally decreased with increasing engine load. For instance, in 2N1S mode, fuel consumption decreased from 439.97 g kWh^{-1} at 25% load to 272.46 g kWh^{-1} at 50% load, reflecting a 38.07% reduction. At 25% load, fuel consumption in Normal and 3N1S modes was 493.93 g kWh^{-1} and 442.24 g kWh^{-1}, respectively.

A decrease in fuel consumption is observed as the engine load increases. In the 2N1S operating mode, while the fuel consumption was 439.97 g kWh^{-1} at 25% engine load, this value decreased by 38.07% to 272.46 g kWh^{-1} at 50% engine load. The reason for the deterioration of the general trend in

3N1S and 2N1S operating modes with engine load change is that more fuel consumption is needed to obtain the same torque. Yüksel et al. [35] studied the effect of different cycle-skipping strategies on engine performance and emissions using an experimental approach. The results show that a 4.3% reduction in fuel consumption is achieved in cycle-skipping strategies compared to normal mode.

Table 5 shows the measured values of carbon monoxide (CO), hydrocarbons (HC), and nitrogen oxides (NO_x) emission values obtained for different engine loads and operating modes. In the study, the emissions from normal operation mode and different operating modes such as 3N1S, 2N1S, and 1N1S were compared. Emission measurements are essential to determine the effect of various operating modes and engine loads on exhaust gas components. Engine load is a primary factor influencing the combustion process, thereby affecting emission characteristics. At lower loads, combustion temperatures are reduced, typically resulting in lower NOx but potentially higher HC and CO emissions. Conversely, at higher loads, elevated temperatures and pressures intensify NOx formation.

The highest CO emission was calculated as 0.534% in the 3N1S operating mode. HC emission was recorded at 128 ppm in the 2N1S mode, whereas it decreased by 2.88% to 91 ppm in the 1N1S mode at a steady engine load of 25%. Increasing engine load generally led to an increase in NOx emissions. In normal mode, raising the load to 50% resulted in a NOx level of 1248 ppm. Baykara et al. [58] investigated the impact of the cycle-skipping strategy on fuel consumption and exhaust emissions under varying engine speeds and operating pressures. The study revealed that the implementation of the cycle-skipping strategy led to a marked increase in NOx emissions, which is considered an unfavorable outcome in terms of environmental impact.

Table 5 Emission values in the engine at different engine loads and operating modes

Cycle-skip mode	Engine load/%	CO/%	HC/ppm	NO_x/ppm
Normal	25	0.018	105	13
	50	0.028	89	72
	75	0.036	115	1320
03N 1S	25	0.026	97	56
	50	0.011	94	1594
	75	0.534	397	1678
2N 1S	25	0.024	128	86
	50	0.051	236	2431
	75	0	0	0
1N 1S	25	0.033	91	2461
	50	0	0	0
	75	0	0	0

Energy flow and heat losses, which are important indicators of engine performance, were calculated for each engine load and operating mode and are summarized in Table 6. In both normal and alternating modes (3N1S, 2N1S, 1N1S), energy input to the engine increased with increasing load. While more energy is generated at higher loads, a portion is inevitably dissipated as heat to the surroundings. Doubling the engine load in normal and 2N1S modes led to increases in thermal losses by 0.944% and 12.006%, respectively. The effect of load on energy flow was more significant in skip modes than in normal mode. In 3N1S operation, the difference in thermal losses between maximum and minimum loads was calculated as 11.052 kW.

Thermal efficiency, based on the first law of thermodynamics, quantifies the portion of input fuel energy converted into mechanical work. High thermal efficiency indicates effective utilization of fuel energy with minimal losses. Figure 5 illustrates the variation of thermal efficiency

Table 6 Energy analysis of the engine at different engine loads and operating modes

Cycle-skip mode	Engine load/%	Energy flow/kW	Heat loss/kW
Normal	25	18.948	14.83
	50	21.309	14.97
	75	27.576	18.15
3N 1S	25	15.713	13.01
	50	20.277	14.91
	75	26.765	19.98
2N 1S	25	13.758	12.91
	50	19.761	14.46
	75	0.000	0.00
1N 1S	25	13.331	9.17
	50	0	0
	75	0	0

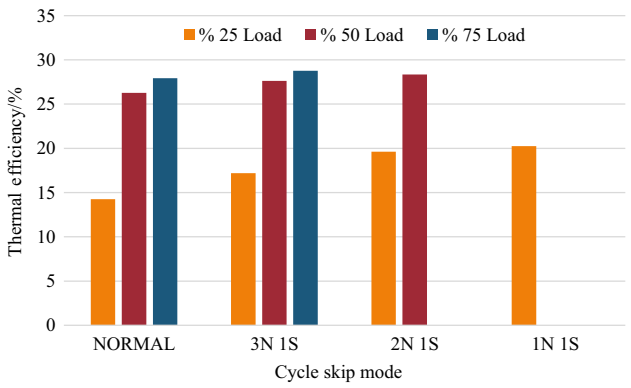

Fig. 5 Thermal efficiency of the engine under varying loads and operational modes

with engine load and operating mode. In normal and 3N1S modes, thermal efficiency increased with load, while 2N1S and 1N1S modes exhibited better performance at low and medium loads. The 2N1S mode is an intermediate strategy that involves two combustion cycles in three. This mode provides a more consistent operation compared to the 1N1S mode. It can meet the required torque, particularly under 50% engine load, while also protecting personnel by reducing pumping losses. This improves combustion stability and achieves efficient power generation.

Both strategies, thanks to cycle-skipping options, allow for complete exhaust gas evacuation during non-combustion cycles and the preparation of fresher mixtures in the next cycle. This contributes to an increase in combustion temperature and exergy temperature. At 25% engine load, thermal efficiency was 14.24% and 20.25% in the normal and 1N1S modes, respectively. The peak thermal efficiency, 28.77%, was recorded at 75% load in the 3N1S mode.

Exergy analysis serves as a diagnostic tool to assess the deviation of the system from ideal thermodynamic behavior, primarily by quantifying irreversibilities. This analysis involves calculating exergy input, exhaust exergy, and thermal exergy losses. The second law (exergy) efficiency, which reflects the quality of energy conversion, was also determined in this study and is presented in Table 7. At higher engine loads, the system releases more heat and when this heat is not distributed evenly in the engine or cannot be recovered effectively, irreversibilities due to heat transfer increase. In the 3N1S mode, the fuel exergy at 75% engine load was found to be 70.37% higher than at 25% engine load.

Exergy flow rates were generally lower under cycle-skipping conditions compared to normal mode. This situation is due to the change in the amount of fuel injected in order to obtain the same torque in the cycle-skip modes. The exergy associated with exhaust gases represents the portion of energy that is unavailable for conversion into useful work. An increase in exhaust exergy was observed under skip modes compared to normal mode.

The cycle-skipping strategy positively influenced combustion by reducing both exhaust and thermal exergy. At 25% engine load, exhaust exergy in the normal mode was 4.85 kW, while it decreased by 9.734% to 4.422 kW in the 1N1S mode. The highest thermal exergy, 3.026 kW, was recorded in the normal mode at 75% load. Conversely, at 25% load, thermal exergy in the 1N1S mode was 49.34% lower than in the normal mode, mainly due to lower exhaust gas temperatures, as illustrated in Fig. 6.

Exergy destruction in the engine results from irreversibilities occurring during energy conversion processes. Minimizing exergy destruction is critical for achieving maximum performance and reducing emissions from a thermodynamic terms. As engine load increases, a greater amount of fuel is introduced into the control volume, leading to higher energy demand. Consequently, fuel consumption rises,

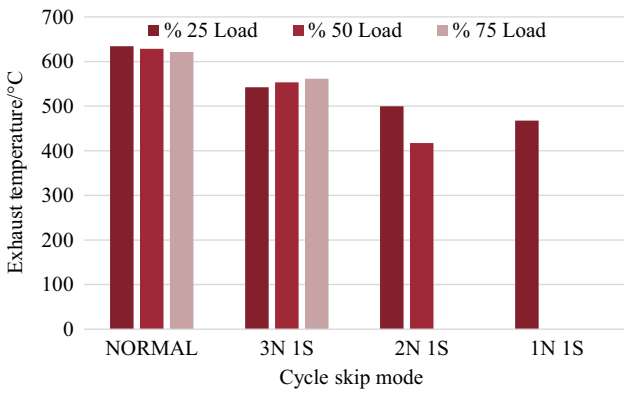

Fig. 6 Exhaust temperatures of the engine under varying loads and operational modes

Table 7 Exergy analysis of the engine at different engine loads and operating modes

Cycle-skip mode	Engine load/%	Exergy flow kW	Exhaust exergy/kW	Heat exergy/kW	Exergy destruction/kW
Normal	25	20.653	4.859	1.893	11.201
	50	23.227	4.703	1.903	11.020
	75	30.058	4.565	3.026	14.767
3N 1S	25	17.127	4.666	1.134	8.627
	50	22.102	4.546	1.688	10.268
	75	29.174	4.424	2.893	14.157
2N 1S	25	14.996	4.530	1.086	6.680
	50	21.539	4.396	1.521	10.022
	75	0	0	0	0
1N 1S	25	14.531	4.422	0.959	6.449
	50	0	0	0	0
	75	0	0	0	0

and thermodynamic irreversibilities become more prominent, thereby increasing exergy losses. In the 3N1S mode, exergy destruction increased from 10.27 kW at 50% load to 14.16 kW at 75% load. At 25% load, the 1N1S mode exhibited 42.41% less exergy destruction compared to the normal operating mode. The highest exergy destruction recorded in the study was 14.77 kW, observed in the normal mode at 75% engine load.

Entropy production and irregularities occurring during the engine operation process cause irreversibility. According to the second law of thermodynamics, every real system produces some entropy, causing energy quality to decrease. Higher entropy production causes more irreversibility and lower engine performance. Therefore, minimizing entropy production is an important issue for maximum engine efficiency. The entropy produced depending on the change of operating modes and engine loads is given in Fig. 7. The 1N1S mode is a strategy that only performs combustion once in every two engine cycles; in this case, combustion events occur once at a crankshaft angle of 1440°. When this strategy is implemented using the HCCI principle, the frequency of combustion decreases and average in-cylinder temperatures decrease. By reducing the frequency of combustion events, temperature changes between successive cycles are limited, reducing thermal gradients and instability in the system. In this study, the 1N1S mode was observed to have the lowest entropy generation at 0.021 kW/K. The 3N1S mode has 4.065% less entropy production at 75% engine load compared to the normal mode without cycle-skip mode.

In the energy conversion stages, not all of the energy can be converted into useful work and some of it loses its usability. According to the second law of thermodynamics, all real processes produce entropy, and increased entropy generation indicates greater thermodynamic inefficiencies and reduced engine performance. Therefore, exergy efficiency represents the quality of energy utilization within the system. In this study conducted on a natural gas-fueled

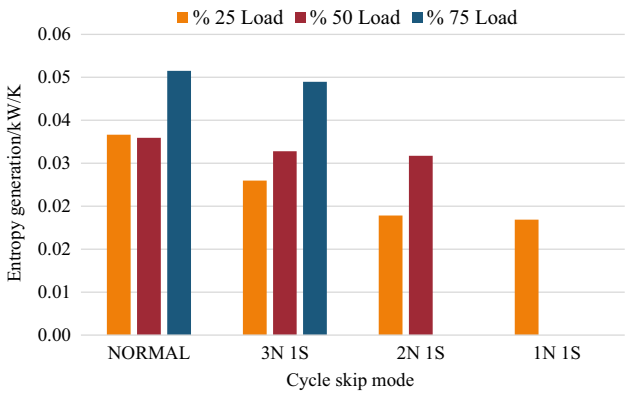

Fig. 7 Entropy production in the engine under varying loads and operational modes

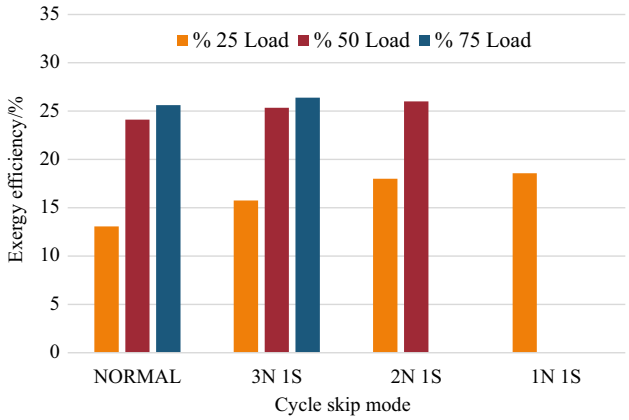

Fig. 8 Exergy efficiency of the engine under varying loads and operational modes

engine, the second law efficiency values for both the normal and alternative operating modes are presented in Fig. 7. The highest exergy efficiency was obtained in the 3N1S operating mode at 75% engine load, with a calculated value of 26.39% is presented in Fig. 8. An improvement in exergy efficiency was observed when transitioning from the normal operating mode to cycle-skipping modes. At an engine load of 25%, the exergy efficiency in the normal operating mode was calculated as 13.073%, whereas this value increased to 18.581% in the 1N1S mode.

Conclusion and discussion

This study conducted performance, emission, exergy, and energy evaluations utilizing experimental data from tests carried out at varying engine loads (25, 50, and 75%) and under distinct operating modes (Normal, 3N1S, 2N1S, and 1N1S) in a natural gas-fueled HCCI engine. The environmental impact of the engine was evaluated by measuring critical emission characteristics, including unused hydrocarbons (HC), nitrogen oxides (NO_x), and carbon monoxide (CO). It was observed that irreversibility increased significantly at high engine loads when the generated heat could not be effectively recovered. In the 3N1S mode, thermal exergy at 75% engine load was 154.97% higher compared to its value at 25% engine load. The maximum fuel exergy was determined as 30.058 kW at 75% engine load under the normal operating mode. Second law (exergy) efficiency, which is one of the most critical indicators of engine performance, increased with rising engine load. While the exergy efficiency in the normal mode at 25% engine load was calculated as 13.073%, this value increased to 18.581% in the 1N1S mode, where the cycle-skipping strategy was applied.

According to the findings, at low engine loads, the 1N1S mode offers a more balanced and optimized operation in

terms of exergy, while at high loads, the 3N1S mode stands out as a more suitable option for increasing system efficiency. This situation highlights the need to develop hybrid strategies based on engine load. Furthermore, integrated cooling systems or waste heat utilization technologies could be considered for future studies to reduce irreversibilities in situations where heat recovery potential is high. Future research is recommended to utilize and optimize different alternative fuels in conjunction with cycle-skipping strategies.

Limitations

The effectiveness of skip cycle strategies may vary at different engine speeds. Therefore, during transient conditions (such as sudden acceleration or load increases), delayed ignition, incomplete combustion in the cylinder, or misfires may occur. Evaluating these effects should be addressed in future studies.

References

1. Calam A. An experimental research on the determination of the combustion characteristics of ABE fuel in a port injection HCCI engine. Energy Convers Manage. 2024;321: 119087.
2. Uyumaz A, Kilmen AB, Kaş M. An experimental study of the influences of lacquer thinner addition to gasoline on performance and emissions of a spark ignition engine. Eng Perspect. 2024;4:54–9.
3. Arslan TA, Kocakulak T. A comprehensive review on sirling engines. Eng Persp. 2023;3:42–56.
4. Leach F, Kalghatgi G, Stone R, Miles P. The scope for improving the efficiency and environmental impact of internal combustion engines. Transp Eng. 2020;1: 100005.
5. Bae C, Kim J. Alternative fuels for internal combustion engines. Proc Combust Inst. 2017;36:3389–413.
6. Shukla PC, Belgiorno G, Di Blasio G, Agarwal AK, editors. Alcohol as an Alternative Fuel for Internal Combustion Engines. Springer Singapore: Singapore; 2021. https://doi.org/10.1007/978-981-16-0931-2.
7. Singh AP, Sharma YC, Mustafi NN, Agarwal AK, editors. Alternative Fuels and Their Utilization Strategies in Internal Combustion Engines. Springer Singapore: Singapore; 2020. https://doi.org/10.1007/978-981-15-0418-1.
8. Lopatin OP (2020) Investigation of alternative fuel oxidation kinetics in an internal combustion engine. In: IOP Conference Series Materials Science and Engineering. IOP Publishing
9. Ibrahim GYAM, Atak NN, Dogan B, Yesilyurt MK, Yaman H. A detailed analysis of a diesel engine fueled with diesel fuel-linseed oil biodiesel-ethanol blends in a thermodynamic, economic, and environmental context. CT&F-Ciencia, Tecnol y Futuro. 2023;2023:39–54.
10. Liu H, Yu S, Wang T, Li J, Wang Y. A systematic review on sustainability assessment of internal combustion engines. J Clean Prod. 2024. https://doi.org/10.1016/j.jclepro.2024.141996.
11. Karim HAA, Hannun RM. (2024) A review of the use of hydrogen gas in internal combustion engines. In: AIP Conference Proceedings. AIP Publishing
12. Hamzah AH, Akroot A, Wahhab HAA, Ghazal RM, Alhamd AE, Bdaiwi M. Effects of nano-additives in developing alternative fuel strategy for CI engines: a critical review with a focus on the performance and emission characteristics. Results Eng. 2024;2024:102248.
13. Ramar K, Subbiah G, Almoallim HS. Ammonia-enriched biogas as an alternative fuel in diesel engines: combustion, performance and emission analysis. Fuel. 2024;369: 131755.
14. Dogan B, Yesilyurt MK, Atak NN. An overview concerning the utilization of fusel oil as an alternative fuel in the engine applications. Proc Inst Mech Eng Part E: J Process Mech Eng. 2024;2024:09544089241228940.
15. Almatrafi E, Siddiqui MA. Thermodynamic investigation of a hydrogen enriched natural gas fueled HCCI engine for the efficient production of power, heating, and cooling. Int J Hydrogen Energy. 2024;82:111–22.
16. Nobakht AY, Saray RK, Rahimi A. A parametric study on natural gas fueled HCCI combustion engine using a multi-zone combustion model. Fuel. 2011;90:1508–14.
17. Djermouni M, Ouadha A. Thermodynamic analysis of an HCCI engine based system running on natural gas. Energy Convers Manage. 2014;88:723–31.
18. Xing H, Stuart C, Spence S, Chen H. Alternative fuel options for low carbon maritime transportation: pathways to 2050. J Clean Prod. 2021;297: 126651.
19. Jayabal R. (2024) Effect of hydrogen/sapota seed biodiesel as an alternative fuel in a diesel engine using dual-fuel mode. Process Safety and Environmental Protection. 2024 [cited 2024 May 22]; Available from: https://www.sciencedirect.com/science/article/pii/S0957582024000478?casa_token=F8kCLnuSz1oAAAAA:RqkDf6-QquGQwN7l9WBwDqRl-xwpeVRdwqyvoC3dCR67mE5qyHdhef1XpcJkTW8x4CN7o7yQD96f
20. Kumar A, Pali HS, Kumar M. Evaluation of waste plastic and waste cooking oil as a potential alternative fuel in diesel engine. Next Energy. 2024;5: 100181.
21. M'hamed B, Moustefa HH, Saïdia LM, Muthanna BGN, Mohamad AT, Sidik NAC. Experimental evaluation of the performance of a diesel engine feeding with ethanol/diesel and methanol/diesel. J Adv Res Exp Fluid Mech Heat Transf. 2024;15:14–27.
22. Krakowski R, Witkowski K. Investigating the effects of environmentally friendly additives on the exhaust gas composition and fuel consumption of an internal combustion engine. Appl Sci. 2024;14:2956.
23. Can O, Cinar C, Şahin F (2009) The investigation of the effects of premixed gasoline charge on HCCI-DI engine combustion and exhaust emissions Ön karisimli benzin dolgusunun HCCI-DI motorunda yanma ve egzoz emisyonlarina etkilerinin incelenmesi. Journal of the Faculty of Engineering and Architecture of Gazi University. [cited 2024 Nov 20];24. Available from: https://avesis.gazi.edu.tr/yayin/99e96294-73b1-48d3-b8a7-3f66bc8f0154/the-investigation-of-the-effects-of-premixed-gasoline-charge-on-hcci-di-engine-combustion-and-exhaust-emissions
24. Ghazikhani M, Kalateh MR, Toroghi YK, Dehnavi M. An experimental study on the effect of premixed and equivalence ratios on CO and HC emissions of dual fuel HCCI engine. World Acad Sci Eng Technol. 2009;52:129–35.
25. Zapata-Mina J, Ardebili SMS, Restrepo A, Solmaz H, Calam A, Can Ö. Exergy analysis in a HCCI engine operated with diethyl ether-fusel oil blends. Case Stud Therm Eng. 2022;32: 101899.
26. Tunçer E, Sandalci T, Balcı Ö, Karagöz Y. Natural gas-fueled HCCI engine performance and emission analysis and comparison with SI and spark-assisted operations. Aust J Mech Eng. 2024;2024:1–12.

27. Verma SK, Gaur S, Akram T, Kumar A. Performance characteristic of HCCI engine for different fuels. Mater Today Proc. 2021;47:6030–4.
28. Çelebi S, Haşimoğlu C, Uyumaz A, Halis S, Calam A, Solmaz H, et al. Operating range, combustion, performance and emissions of an HCCI engine fueled with naphtha. Fuel. 2021;283: 118828.
29. Polat S. An experimental investigation on combustion, performance and ringing operation characteristics of a low compression ratio early direct injection HCCI engine with ethanol fuel blends. Fuel. 2020;277: 118092.
30. Pochet M, Jeanmart H, Contino F. A 22: 1 compression ratio ammonia-hydrogen HCCI engine: combustion, load, and emission performances. Front Mech Eng. 2020;6:43.
31. Telli GD, Zulian GY, Lanzanova TDM, Martins MES, Rocha LAO. An experimental study of performance, combustion and emissions characteristics of an ethanol HCCI engine using water injection. Appl Therm Eng. 2022;204: 118003.
32. Elkelawy M, Alm ElDin Mohamad H, Abd Elhamid E, El-Gamal MA. A critical review of the performance, combustion, and emissions characteristics of PCCI engine controlled by injection strategy and fuel properties. J Eng Res. 2022;6:96–110.
33. Bukkarapu KR, Krishnasamy A. Evaluating the feasibility of machine learning algorithms for combustion regime classification in biodiesel-fueled homogeneous charge compression ignition engines. Fuel. 2024;374: 132406.
34. Kutlar OA, Arslan H, Calik AT. Skip cycle system for spark ignition engines: an experimental investigation of a new type working strategy. Energy Convers Manage. 2007;48:370–9.
35. Dogru B, Lot R, Dinesh KR. Valve timing optimisation of a spark ignition engine with skip cycle strategy. Energy Convers Manag. 2018;173:95–112.
36. Yüksek L, Özener O, Sandalcı T. Cycle-skipping strategies for pumping loss reduction in spark ignition engines: an experimental approach. Energy Convers Manage. 2012;64:320–7.
37. Vikraman V, Anand K, Ramesh A. Novel strategies to overcome the limitations of a low compression ratio light duty diesel engine. Int J Engine Res. 2021;22:2830–51.
38. Wang J, Duan X, Wang W, Guan J, Li Y, Liu J. Effects of the continuous variable valve lift system and Miller cycle strategy on the performance behavior of the lean-burn natural gas spark ignition engine. Fuel. 2021;297: 120762.
39. Gürbüz H. Simulation analysis of cycle skipping strategy in SI engine fueled with ethanol gasoline mixture. Int J Automot Eng Technol. 2023;12:51–6.
40. Tunçer E, Doğan B, Sandalcı T, Erol D. Energy and exergy analyses of skipped cycle mode in a single-cylinder engine fuelled with diesel and natural gas. IJEX. 2022;39:173.
41. Tunçer E, Sandalci T, Pusat S, Balcı Ö, Karagöz Y. Cycle-skipping strategy with intake air cut off for natural gas fueled Si engine. Sci Prog. 2021;104:00368504211031074.
42. Korakianitis T, Namasivayam AM, Crookes RJ. Natural-gas fueled spark-ignition (SI) and compression-ignition (CI) engine performance and emissions. Prog Energy Combust Sci. 2011;37:89–112.
43. Ryu K. Effects of pilot injection pressure on the combustion and emissions characteristics in a diesel engine using biodiesel–CNG dual fuel. Energy Convers Manage. 2013;76:506–16.
44. Pathak SK, Nayyar A, Goel V. Optimization of EGR effects on performance and emission parameters of a dual fuel (Diesel+ CNG) CI engine: an experimental investigation. Fuel. 2021;291: 120183.
45. Bharathiraja M, Venkatachalam R, Senthilmurugan V. Performance, emission, energy and exergy analyses of gasoline fumigated DI diesel engine. J Therm Anal Calorim. 2019;136:281–93.
46. Yesilyurt MK. The examination of a compression-ignition engine powered by peanut oil biodiesel and diesel fuel in terms of energetic and exergetic performance parameters. Fuel. 2020;278: 118319.
47. Şanli BG, Uludamar E, Özcanli M. Evaluation of energetic-exergetic and sustainability parameters of biodiesel fuels produced from palm oil and opium poppy oil as alternative fuels in diesel engines. Fuel. 2019;258: 116116.
48. Dogan B, Cakmak A, Yesilyurt MK, Erol D. Investigation on 1-heptanol as an oxygenated additive with diesel fuel for compression-ignition engine applications: an approach in terms of energy, exergy, exergoeconomic, enviroeconomic, and sustainability analyses. Fuel. 2020;275: 117973.
49. Kumar R. A critical review on energy, exergy, exergoeconomic and economic (4-E) analysis of thermal power plants. Eng Sci Technol Int J. 2017;20:283–92.
50. Hepbasli A, Akdemir O. Energy and exergy analysis of a ground source (geothermal) heat pump system. Energy Convers Manag. 2004;45:737–53.
51. Salek F, Babaie M, Ghodsi A, Hosseini SV, Zare A. Energy and exergy analysis of a novel turbo-compounding system for supercharging and mild hybridization of a gasoline engine. J Therm Anal Calorim. 2021;145:817–28.
52. Şanli BG. Energetic and exergetic performance of a diesel engine fueled with diesel and microalgae biodiesel. Energy Sources Part A Recover Util Environ Eff. 2019;41:2519–33.
53. Karagoz M, Uysal C, Agbulut U, Saridemir S. Energy, exergy, economic and sustainability assessments of a compression ignition diesel engine fueled with tire pyrolytic oil- diesel blends. J Clean Prod. 2020;264: 121724.
54. Moran MJ, Shapiro HN, Boettner DD, Bailey MB. Fundamentals of engineering thermodynamics. UK: John Wiley & Sons; 2010.
55. Doğan B, Erol D, Yaman H, Kodanli E. The effect of ethanol-gasoline blends on performance and exhaust emissions of a spark ignition engine through exergy analysis. Appl Therm Eng. 2017;120:433–43.
56. Caliskan H, Mori K. Environmental, enviroeconomic and enhanced thermodynamic analyses of a diesel engine with diesel oxidation catalyst (DOC) and diesel particulate filter (DPF) after treatment systems. Energy. 2017;128:128–44.
57. Doğan B, Erol D, Kodanlı E. The investigation of exergoeconomic, sustainability and environmental analyses in an SI engine fuelled with different ethanol-gasoline blends. IJEX. 2020;32:412.
58. Baykara C, Kutlar OA, Dogru B, Arslan H. Skip cycle method with a valve-control mechanism for spark ignition engines. Energy Convers Manage. 2017;146:134–46.